proceedings

MDPI

Proceedings

$CsPbBr_3$ Perovskite Nanocrystal/S Doping g-C_3N_4 Ultra-Thin Nanosheet Heterojunction with Enhanced Interfacial Charge Transfer for Photocatalytic CO_2 Reduction †

Tianyu Zhao, Deyang Li, Yiyan Zhang and Guanying Chen *

School of Chemistry and Chemical Engineering, Harbin Institute of Technology, Harbin 150001, China

* Correspondence: chenguanying@hit.edu.cn

† Presented at the 2nd International Online-Conference on Nanomaterials, 15–30 November 2020; Available online: https://iocn2020.sciforum.net/.

Published: 15 November 2020

Abstract: A single paragraph of about 200 words maximum. For research articles, abstracts should give a pertinent overview of the work. We strongly encourage authors to use the following style of structured abstracts, but without headings: (1) Background: Place the question addressed in a broad context and highlight the purpose of the study; (2) Methods: Describe briefly the main methods or treatments applied; (3) Results: Summarize the article's main findings; and (4) Conclusions: Indicate the main conclusions or interpretations. The abstract should be an objective representation of the article, it must not contain results which are not presented and substantiated in the main text and should not exaggerate the main conclusions.

Keywords: perovskite; photocatalysis; g-C_3N_4; CO_2; quantum dots

1. Introduction

At present, a large number of fossil fuel consumption has led to a series of energy shortages and environmental problems [1,2]. As the main combustion product, carbon dioxide (CO_2) is the main contributor to climate warming, which is usually discharged into the atmosphere without treatment. In order to alleviate the above environmental problems, people are committed to the capture, storage and utilization of CO_2 [3–6]. Using CO_2 as a carbon source to synthesize valuable products is considered to be an effective way to solve the problems of climate warming and energy shortage [7–9]. In the current process of energy conversion, the photocatalytic reduction of CO_2 light into high-energy products is considered a sustainable, green, but challenging strategy [10–12].

As a polymeric photocatalyst composed of earth-abundant elements, graphitic carbon nitride (g-C_3N_4) with nontoxicity, excellent physical/chemical stability, appropriate energy band, and low cost has emerged as a rather promising candidate for photocatalytic degradation [13–15], photocatalytic H_2 evolution [16–19], photocatalytic CO_2 reduction [20–22] and so on. However, due to the rapid recombination and the low mobility of photogenerated charge carriers, relatively narrow visible light responsive region, and the small specific surface area, the photocatalytic performance of bulk g-C_3N_4 with highly stacked layers is not ideal [23]. Therefore, in order to improve the photocatalytic performance, many methods (such as: element doping, constructing heterostructures and morphology control) have been proposed to promote the transport and separation of photogenerated carriers and increase the specific surface area [24,25]. Recently, due to the control of molecular structure, the introduction of anions into the g-C_3N_4 framework has been shown to significantly enhance the intrinsic activity of g-C_3N_4 [23]. Nonmetal doping not only increases the separation rate

of photogenerated charge carrier, but also enhances the visible-light absorption of g-C_3N_4 [26]. Previous research has mainly focused on single-element doping. However, compared with single-element doping, two non-metallic atoms doped into g-C_3N_4 simultaneously have higher photocatalytic activity and unusual physical and chemical properties. Furthermore, the photocatalytic performance of g-C_3N_4 can be improved by changing the bulk g-C_3N_4 into the layered g-C_3N_4 structure, which is due to the larger specific surface area and more exposed active sites of the layered structure [27–29].

Lead halide perovskite materials have attracted wide interest in photovoltaic and optoelectronic applications due to their unique optical properties [30]. In recent years, due to its visible light absorption, high extinction coefficient, long electron and hole diffusion length, halide perovskites have become ideal materials for optoelectronic applications, especially in photovoltaic devices [31] and light emitting diode [32]. Recently, because lead halide perovskite has a suitable energy band structure, it has also been widely studied as a photocatalytic material for photocatalytic H_2 evolution [33,34] and photocatalytic CO_2 reduction [35,36]. However, the conversion efficiency of pristine lead halide perovskite is not ideal due to the rapid recombination of electron hole pairs, the lack of active centers and chemical instability. heterostructure integrated lead halide perovskite and ultra-thin two-dimensional (2D) material with high specific surface area, rich active centers and strong interface contact, is a very attractive photocatalyst of photocatalytic CO_2 reduction. It's well known that the transfer and separation of photogenerated charge is the key issue in the process of photocatalysis.

Herein, we use a facile method to generate $CsPbBr_3$ in situ on S doped g-C_3N_4 (CPB/USCN). The CPB/USCN photocatalyst exhibited high photocatalytic CO_2 reduction under visible light. In addition, the detailed structure of CPB/USCN and a possible photocatalytic mechanism are discussed through experiments and characterization results.

2. Result and Discussion

The structure of the catalyst is characterized by TEM. As shown in Figure 1a, it can be seen that the small particle size $CsPbBr_3$ is loaded on the surface of ultra-thin g-C_3N_4 nanosheets to form the composite. In addition, it can be clearly seen from Figure 1b that the lattice fringes of a are 0.41 nm, corresponding to (101) plane of cubic $CsPbBr_3$. The morphology of CPB/USCN is further characterized by AFM. As shown in Figures 1d and e, the thickness of the sheet is about 2.5 nm, which strongly proves the formation of ultrathin layered structure. In addition, it is clear from Figure 1c,f that the composite is successfully formed, and the properties of $CsPbBr_3$ and g-C_3N_4 do not change after forming the composite.

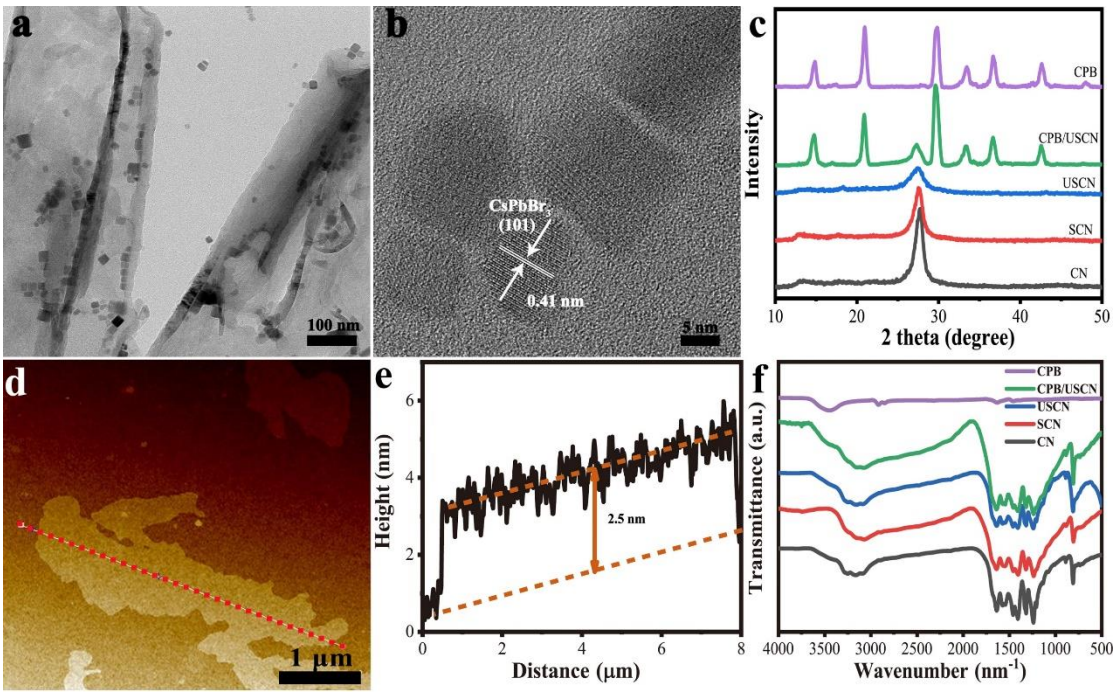

Figure 1. TEM (**a**) and HRTEM image (**b**). AFM of ultra-thin S doping g-C_3N_4 (**d**,**e**). XRD patterns (**c**) and FTIR spectra (**f**) of as-prepared samples.

The photocatalytic CO_2 reduction efficiency of CPB, CN, SCN, and CPB/USCN is evaluated under visible light irradiation. As shown in Figure 2a, the CPB/USCN exhibits the highest photocatalytic activity, which is due to the formation of heterostructures and S doping. In addition, as shown in Figure 2b, the stability of the photocatalyst is also evaluated. After 4 cycles, it still maintained good photocatalytic performance, which indicated that the photocatalyst had good photocatalytic stability. Based on the above results, a possible photocatalytic mechanism is proposed. As shown in Figure 3, $CsPbBr_3$ and S-doping g-C_3N_4 form type II heterojunction. Under visible light irradiation, photogenerated electrons transfer from the conduction band of $CsPbBr_3$ to the conduction band of USCN, and holes transfer from the valence band of USCN to the valence band of $CsPbBr_3$. The formation of heterostructure promotes the separation and transmission of photogenerated carriers. Through the formation of heterojunction and S doping to suppress the recombination of carriers, better photocatalytic performance is obtained.

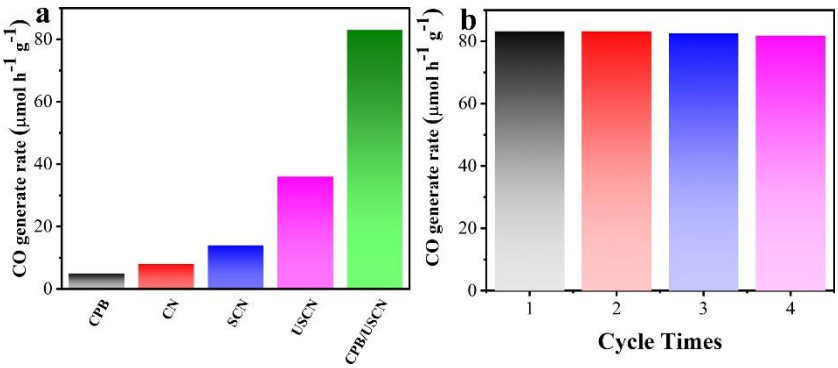

Figure 2. The photocatalytic CO^2 reduction rate of as-prepared samples (**a**). The cycle stability experiment (**b**).

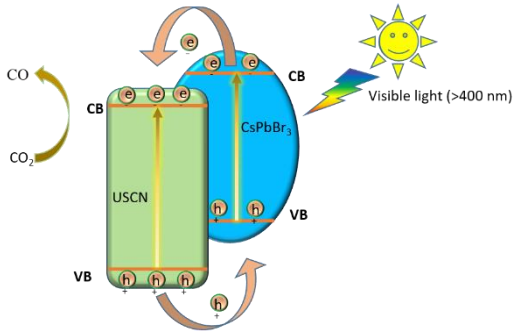

Figure 3. Possible photocatalytic mechanism under visible light irradiation.

3. Conclusions

The novel $CsPbBr_3$ quantum dots/S doping g-C_3N_4 ultrathin nanosheet 0D/2D heterojunctions photocatalyst were prepared by loading perovskite quantum dots onto the surface of ultrathin doped g-C_3N_4. The strategy of S element doping improved the properties of in g-C_3N_4 ultra-thin structure providing more adsorption and reaction sites for photocatalytic CO_2 reduction activity.

4. Method

Bulk g-C_3N_4 was synthesized by calcining melamine S doping g-C_3N_4 ultra-thin nanosheets was synthesized by secondary calcination melamine and thiourea. The $CsPbBr_3$/S doping g-C_3N_4 ultra-thin nanosheets heterostructure was fabricated by an in-situ thermal injection method.

Conflicts of Interest: The authors declare no conflict of interest.

References

1. Singh, G.; Lee, J.; Karakoti, A.; Bahadur, R.; Yi, J.; Zhao, D.; AlBahily, K.; Vinu, A. Emerging trends in porous materials for CO_2 capture and conversion. *Chem. Soc. Rev.* **2020**, *49*, 4360–4404.
2. Das, S.; Pérez-Ramírez, J.; Gong, J.; Dewangan, N.; Hidajat, K.; Gates, B.C.; Kawi, S. Core–shell structured catalysts for thermocatalytic, photocatalytic, and electrocatalytic conversion of CO_2. *Chem. Soc. Rev.* **2020**, *49*, 2937–3004.
3. Talapaneni, S.N.; Singh, G.; Kim, I.Y.; AlBahily, K.; Al-Muhtaseb, A.A.H.; Karakoti, A.S.; Tavakkoli, E.; Vinu, A. Nanostructured Carbon Nitrides for CO_2 Capture and Conversion. *Adv. Mater.* **2019**, *32*, e1904635.
4. Wu, Y.; Cao, S.; Hou, J.; Li, Z.; Zhang, B.; Zhai, P.; Zhang, Y.; Sun, L. Rational Design of Nanocatalysts with Nonmetal Species Modification for Electrochemical CO_2 Reduction. *Adv. Energy Mater.* **2020**, *10*, 2000588.
5. Popović, S.; Smiljanić, M.; Jovanovič, P.; Vavra, J.; Buonsanti, R.; Hodnik, N. Stability and Degradation Mechanisms of Copper-Based Catalysts for Electrochemical CO_2 Reduction. *Angew. Chem. Int. Ed.* **2020**, *132*, 14844–14854.
6. Guo, S.; Zhao, S.; Wu, X.; Li, H.; Zhou, Y.; Zhu, C.; Yang, N.; Jiang, X.; Gao, J.; Bai, L.; et al. A Co_3O_4-CDots-C_3N_4 three component electrocatalyst design concept for efficient and tunable CO_2 reduction to syngas. *Nat. Commun.* **2017**, *8*, 1828.
7. Prabhu, P.; Jose, V.; Lee, J.-M. Heterostructured Catalysts for Electrocatalytic and Photocatalytic Carbon Dioxide Reduction. *Adv. Funct. Mater.* **2020**, *30*, 1910768.
8. Wang, S.; Hai, X.; Ding, X.; Jin, S.; Xiang, Y.; Wang, P.; Jiang, B.; Ichihara, F.; Oshikiri, M.; Meng, X.; et al. Intermolecular cascaded π-conjugation channels for electron delivery powering CO_2 photoreduction. *Nat. Commun.* **2020**, *11*, 1149.
9. Wu, Y.A.; McNulty, I.; Liu, C.; Lau, K.C.; Liu, Q.; Paulikas, A.P.; Sun, C.-J.; Cai, Z.; Guest, J.R.; Ren, Y.; et al. Facet-dependent active sites of a single Cu_2O particle photocatalyst for CO_2 reduction to methanol. *Nat. Energy* **2019**, *4*, 957–968.
10. Wang, Y.; Shang, X.; Shen, J.; Zhang, Z.; Wang, D.; Lin, J.; Wu, J.C.S.; Fu, X.; Wang, X.; Li, C. Direct and indirect Z-scheme heterostructure-coupled photosystem enabling cooperation of CO_2 reduction and H_2O oxidation. *Nat. Commun.* **2020**, *11*, 3043.

11. Zhao, F.; Feng, Y.; Wang, Y.; Zhang, X.; Liang, X.; Li, Z.; Zhang, F.; Wang, T.; Gong, J.; Feng, W. Two-dimensional gersiloxenes with tunable bandgap for photocatalytic H_2 evolution and CO_2 photoreduction to CO. *Nat. Commun.* **2020**, *11*, 1443.
12. He, J.; Janáky, C. Recent Advances in Solar-Driven Carbon Dioxide Conversion: Expectations versus Reality. *ACS Energy Lett.* **2020**, *5*, 1996–2014.
13. Ye, M.-Y.; Zhao, Z.-H.; Hu, Z.-F.; Liu, L.-Q.; Ji, H.-M.; Shen, Z.-R.; Ma, T.-Y. 0D/2D Heterojunctions of Vanadate Quantum Dots/Graphitic Carbon Nitride Nanosheets for Enhanced Visible-Light-Driven Photocatalysis. *Angew. Chem. Int. Ed.* **2017**, *56*, 8407–8411.
14. Yu, Y.; Xu, W.; Fang, J.; Chen, D.; Pan, T.; Feng, W.; Liang, Y.; Fang, Z. Soft-template assisted construction of superstructure $TiO_2/SiO_2/g\text{-}C_3N_4$ hybrid as efficient visible-light photocatalysts to degrade berberine in seawater via an adsorption-photocatalysis synergy and mechanism insight. *Appl. Catal. B Environ.* **2020**, *268*, 118751.
15. Hu, J.; Zhang, P.; An, W.; Liu, L.; Liang, Y.; Cui, W. In-situ Fe-doped $g\text{-}C_3N_4$ heterogeneous catalyst via photocatalysis-Fenton reaction with enriched photocatalytic performance for removal of complex wastewater. *Appl. Catal. B Environ.* **2019**, *245*, 130–142.
16. Wang, Y.; Liu, X.; Liu, J.; Han, B.; Hu, X.; Yang, F.; Xu, Z.; Li, Y.; Jia, S.; Li, Z.; et al. Carbon Quantum Dot Implanted Graphite Carbon Nitride Nanotubes: Excellent Charge Separation and Enhanced Photocatalytic Hydrogen Evolution. *Angew. Chem. Int. Ed.* **2018**, *57*, 5765–5771.
17. Wen, P.; Zhao, K.; Li, H.; Li, J.; Li, J.; Ma, Q.; Geyer, S.M.; Jiang, L.; Qiu, Y. In situ decorated Ni_2P nanocrystal co-catalysts on $g\text{-}C_3N_4$ for efficient and stable photocatalytic hydrogen evolution via a facile co-heating method. *J. Mater. Chem. A* **2020**, *8*, 2995–3004.
18. Zhu, M.; Kim, S.; Mao, L.; Fujitsuka, M.; Zhang, J.; Wang, X.; Majima, T. Metal-Free Photocatalyst for H_2 Evolution in Visible to Near-Infrared Region: Black Phosphorus/Graphitic Carbon Nitride. *J. Am. Chem. Soc.* **2017**, *139*, 13234–13242.
19. Tong, Z.; Yang, D.; Li, Z.; Nan, Y.; Ding, F.; Shen, Y.; Jiang, Z. Thylakoid-Inspired Multishell $g\text{-}C_3N_4$ Nanocapsules with Enhanced Visible-Light Harvesting and Electron Transfer Properties for High-Efficiency Photocatalysis. *ACS Nano* **2017**, *11*, 1103–1112.
20. Wang, S.; Zhan, J.; Chen, K.; Ali, A.; Zeng, L.; Zhao, H.; Hu, W.; Zhu, L.; Xu, X. Potassium-Doped $g\text{-}C_3N_4$ Achieving Efficient Visible-Light-Driven CO_2 Reduction. *ACS Sustain. Chem. Eng.* **2020**, *8*, 8214–8222.
21. Chen, Y.; Wang, F.; Cao, Y.; Zhang, F.; Zou, Y.; Huang, Z.; Ye, L.; Zhou, Y. Interfacial Oxygen Vacancy Engineered Two-Dimensional $g\text{-}C_3N_4$/BiOCl Heterostructures with Boosted Photocatalytic Conversion of CO_2. *ACS Appl. Energy Mater.* **2020**, *3*, 4610–4618.
22. Xu, G.; Zhang, H.; Wei, J.; Zhang, H.-X.; Wu, X.; Li, Y.; Li, C.; Zhang, J.; Ye, J. Integrating the $g\text{-}C_3N_4$ Nanosheet with B–H Bonding Decorated Metal–Organic Framework for CO_2 Activation and Photoreduction. *ACS Nano* **2018**, *12*, 5333–5340.
23. Long, D.; Chen, Z.; Rao, X.; Zhang, Y. Sulfur-Doped $g\text{-}C_3N_4$ and $BiPO_4$ Nanorod Hybrid Architectures for Enhanced Photocatalytic Hydrogen Evolution under Visible Light Irradiation. *ACS Appl. Energy Mater.* **2020**, *3*, 5024–5030.
24. He, F.; Wang, Z.; Li, Y.; Peng, S.; Liu, B. The nonmetal modulation of composition and morphology of $g\text{-}C_3N_4$-based photocatalysts. *Appl. Catal. B Environ.* **2020**, *269*, 118828.
25. Zhang, Q.; Huang, S.; Deng, J.; Gangadharan, D.T.; Yang, F.; Xu, Z.; Giorgi, G.; Palummo, M.; Chaker, M.; Ma, D. Ice-Assisted Synthesis of Black Phosphorus Nanosheets as a Metal-Free Photocatalyst: 2D/2D Heterostructure for Broadband H_2 Evolution. *Adv. Funct. Mater.* **2019**, *29*, 1902486.
26. Hu, X.; Zhang, W.; Yong, Y.; Xu, Y.; Wang, X.; Yao, X. One-step synthesis of iodine-doped $g\text{-}C_3N_4$ with enhanced photocatalytic nitrogen fixation performance. *Appl. Surf. Sci.* **2020**, *510*, 145413.
27. Sun, X.; Huang, H.; Zhao, Q.; Ma, T.; Wang, L. Thin-Layered Photocatalysts. *Adv. Funct. Mater.* **2016**, *30*, 1910005.
28. Xiao, Y.; Tian, G.; Li, W.; Xie, Y.; Jiang, B.; Tian, C.; Zhao, D.; Fu, H. Molecule Self-Assembly Synthesis of Porous Few-Layer Carbon Nitride for Highly Efficient Photoredox Catalysis. *J. Am. Chem. Soc.* **2019**, *141*, 2508–2515.
29. Niu, P.; Zhang, L.; Liu, G.; Cheng, H.-M. Graphene-Like Carbon Nitride Nanosheets for Improved Photocatalytic Activities. *Adv. Funct. Mater.* **2012**, *22*, 4763–4770.

30. Protesescu, L.; Yakunin, S.; Bodnarchuk, M.I.; Krieg, F.; Caputo, R.; Hendon, C.H.; Yang, R.X.; Walsh, A.; Kovalenko, M.V. Nanocrystals of Cesium Lead Halide Perovskites ($CsPbX_3$, X = Cl, Br, and I): Novel Optoelectronic Materials Showing Bright Emission with Wide Color Gamut. *Nano Lett.* **2015**, *15*, 3692–3696.
31. Li, S.-X.; Xu, Y.-S.; Li, C.-L.; Guo, Q.; Wang, G.; Xia, H.; Fang, H.-H.; Shen, L.; Sun, H.-B. Perovskite Single-Crystal Microwire-Array Photodetectors with Performance Stability beyond 1 Year. *Adv. Mater.* **2020**, *32*, e2001998.
32. Wang, H.; Zhang, X.; Wu, Q.; Cao, F.; Yang, D.; Shang, Y.; Ning, Z.; Zhang, W.; Zheng, W.; Yan, Y.; et al. Trifluoroacetate induced small-grained $CsPbBr_3$ perovskite films result in efficient and stable light-emitting devices. *Nat. Commun.* **2019**, *10*, 665.
33. Wu, Y.; Wang, P.; Guan, Z.; Liu, J.; Wang, Z.; Zheng, Z.; Jin, S.; Dai, Y.; Whangbo, M.-H.; Huang, B. Enhancing the Photocatalytic Hydrogen Evolution Activity of Mixed-Halide Perovskite $CH_3NH_3PbBr_{3-x}I_x$ Achieved by Bandgap Funneling of Charge Carriers. *ACS Catal.* **2018**, *8*, 10349–10357.
34. Xiao, M.; Hao, M.; Lyu, M.; Moore, E.G.; Zhang, C.; Luo, B.; Hou, J.; Lipton-Duffin, J.; Wang, L. Surface Ligands Stabilized Lead Halide Perovskite Quantum Dot Photocatalyst for Visible Light-Driven Hydrogen Generation. *Adv. Funct. Mater.* **2019**, *29*, 1905683.
35. Kumar, S.; Regue, M.; Isaacs, M.A.; Freeman, E.; Eslava, S. All-Inorganic $CsPbBr_3$ Nanocrystals: Gram-Scale Mechanochemical Synthesis and Selective Photocatalytic CO_2 Reduction to Methane. *ACS Appl. Energy Mater.* **2020**, *3*, 4509–4522.
36. Wang, X.-D.; Huang, Y.-H.; Liao, J.-F.; Jiang, Y.; Zhou, L.; Zhang, X.-Y.; Chen, H.-Y.; Kuang, D.-B. In Situ Construction of a Cs_2SnI_6 Perovskite Nanocrystal/SnS2 Nanosheet Heterojunction with Boosted Interfacial Charge Transfer. *J. Am. Chem. Soc.* **2019**, *141*, 13434–13441.